Chemometrics tools for investigating complex synchrotron radiation FTIR micro-spectra: focus on historical bowed musical instruments

Giacomo Fiocco[1,2], Silvia Grassi[3], Claudia Invernizzi[1,4], Tommaso Rovetta[1], Michela Albano[1,5], Patrizia Davit[2], Monica Gulmini[2], Chiaramaria Stani[6,7], Lisa Vaccari[6], Maurizio Licchelli[1], Marco Malagodi[1,8]

[1] *Arvedi Laboratory of Non-Invasive Diagnostics, CISRiC, Università degli Studi di Pavia, Via Bell'Aspa 3, 26100 Cremona, Italy*
[2] *Department of Chemistry, Università di Torino, Via Pietro Giuria 7, 10125, Torino, Italy*
[3] *Department of Food, Environmental, and Nutritional Sciences, Università degli Studi di Milano, via G. Celoria 2, 20133 Milan, Italy*
[4] *Department of Mathematical, Physical and Computer Sciences, Università di Parma, Parco Area delle Scienze 7/A, 43124 Parma, Italy*
[5] *Department of Physics, Polytechnic of Milan, Piazza Leonardo da Vinci 32, 20133, Milano, Italy*
[6] *Elettra-Sincrotrone Trieste S.C.p.A., S.S. 14 km 163.5, 34194 Basovizza, Trieste, Italy*
[7] *CERIC-ERIC, S.S. 14 km 163.5, 34194 Basovizza, Trieste, Italy*
[8] *Department of Musicology and Cultural Heritage, Università degli Studi di Pavia, Corso Garibaldi 178, 26100 Cremona, Italy*

ABSTRACT
The investigation of the coating systems used on historical bowed string musical instruments is generally highly complex due to the coatings' reduced thickness and multi-layered structure. Furthermore, sampling is rarely feasible, and non-invasive approaches do not always allow researchers to undertake a thorough characterisation. Thus, in the rare cases of availability, the opportunity must be taken to investigate the best micro-samples in detail using a suite of analytical spectroscopic techniques that allow for obtaining various informative spectra. Their subsequent interpretation should lead to the characterisation of the finishing layers, the preparation of which involves a careful selection of organic and inorganic compounds.
In the present work, synchrotron radiation and micro-Fourier-transform infrared spectroscopy were combined in terms of reflection geometry and chemometrics to investigate six cross-sectioned micro-samples detached from four bowed string instruments produced by Antonio Stradivari, Francesco Ruggeri, and Lorenzo Storioni. Various chemometric tools enabled us to perform a preliminary exploration of the entire collected infrared dataset, while a classification model based on partial least squares–discriminant analysis was used to discriminate the materials through the characteristic signals. High model specificity (> 0.9) was achieved in the prediction, providing the groundwork for the application of a fast and rigorous methodological approach.

Corresponding author: Monica Gulmini, e-mail: monica.gulmini@unito.it

1. INTRODUCTION

During the last decade, an increasing number of historical bowed string instruments have been investigated, with a large suite of analytical techniques being employed by the researchers to discover the secrets of these masterpieces of craftsmanship [1],[2]. Here, the research was mainly focused on the nature of the precious varnish [3]-[5] and of the other materials involved in the finishing treatments used by the Cremonese violin makers [6],[7]. Generally, multiple thin varnish layers (a few microns of thickness) were applied on the wood, which was previously treated with a sealer and covered by a ground coat to prevent varnish penetration [8]. In addition, micrometric inorganic particles were often dispersed in the coatings [9],[10]. The most common materials involved in the finishing processes were

siccative oils, natural resins, casein or animal glue, inorganic fillers (e.g. calcium carbonate, gypsum, silicates), and pigments (both organic and inorganic) [11]-[13].

The scientific investigations in this field, generally highly challenging due to the intrinsic complexity of the coating systems, are rendered even more arduous due to the large variety of unknown restoration materials that could have been laid on top of the original materials over time [14].

In addition, given the high value of the historical musical instruments, sampling is rarely allowed. In the rare case where a micro-sample can be taken from the surface, it is generally embedded in epoxy resin and then cut as a cross section [15]. Here, to obtain the maximum amount of information, researchers must collect a large amount of data using a suite of analytical techniques. While a non-invasive approach is generally preferred [16], a combination of non- and micro-invasive spectroscopic techniques is often used to comprehensively characterise the historical materials, generally in conjunction with various imaging, tomographic, and chromatographic techniques [17]-[21].

In recent years, the use of chemometrics in the field of heritage science has been tested for an in-depth elaboration of large datasets [22]. These analytical tools are largely employed to support a preliminary interpretation of the spectroscopic results and to improve the visual representation of the information carried by the spectra [23].

In this work, six micro-samples mounted in various cross sections were analysed using synchrotron radiation (SR)–Fourier transform infrared (FTIR) micro-spectroscopy at Elettra Sincrotrone Trieste (Source for Imaging and Spectroscopic Studies in the Infrared [SISSI] beamline, Chemical and Life Sciences branch) [24]. The samples were detached from four historical bowed string instruments made in Cremona by Antonio Stradivari (1644–1737), Francesco Ruggeri 'il Per' (1630–1698), and Lorenzo Storioni (1744–1816) [25]. To preserve the surface of these unique cross sections such that further analyses can be developed in the future, a micro-attenuated total reflection mode was excluded [26], with the spectra collected in reflection geometry ensure that the objective did not come into contact with the samples. The SR technique increased the lateral resolution and signal-to-noise ratio [27],[28], allowing us to set the analytical spot up to the minimum layer thickness of 10 μm.

Despite the constraints imposed by the sampling geometry and by the reduced layer thickness, numerous complex spectra were derived from the cross sections. While this analytical approach is promising for achieving the characterisation of the coating system, a huge amount of effort is required to obtain a reliable and rigorous preliminary picture of the information hidden in the entire infrared (IR) dataset. Consequently, to support the data-processing step in view of extending the use of this analytical technique to a larger number of samples, and to

obtain as much information as possible from the analyses, it was decided to process the spectra using a multivariate approach. In fact, various chemometric tools are generally used to elaborate the data from a multivariate point of view, which allows for unravelling the relevant information carried by the spectroscopic signals in terms of, for example, SR–FTIR spectra. Specifically, through the use of an unsupervised exploratory procedure, namely, principal component analysis (PCA), it is possible to understand the relationship between all the variables and to extract the sample patterns according to the weight of the variables in a new reduced space defined by the PC components [29],[30]. Moreover, supervised classification methods (e.g. linear discriminant analysis, partial least squares–discriminant analysis [PLS–DA], support vector machines, artificial neural networks) enable the definition of rules aimed at distinguishing objects into classes, such as different materials, which allows for material classification and for skipping the visual inspection of the large number of spectra.

Within this context, the present work aimed to (i) develop a multivariate methodological framework for managing and interpreting large IR datasets and subsequently (ii) compare and describe the spectra collected for the six micro-samples using the chemometric tools, namely, PCA and PLS–DA.

The remainder of the paper is organised as follows. In section 2, the musical instruments considered in the research, the micro-sampling, and the embedding method are described, while the procedures used during the SR–FTIR micro-spectroscopic analyses are explained together with the chemometrics approach and the attendant procedures. In section 3, the expected IR bands and the results obtained via PCA from the IR dataset exploration are presented and discussed alongside the classification results obtained via PLS–DA modelling. Finally, the findings are summarised and potential future research directions are outlined in section 4.

2. MATERIALS AND METHODS

The experimental plan encompassed the analysis of six sub-millimetric samples collected from four different bowed string instruments (Table 1): a fragment of a cello made by Francesco Ruggeri during the 17th Century (FR_c), the Toscano violin made by Antonio Stradivari in 1690 (AS_v), and the Bracco small violin (LS_sv1, LS_sv2 and LS_sv3) and a small privately owned violin (LS_v), which were made by Lorenzo Storioni in 1793 and 1790, respectively. The samples were collected under high magnification, employing a disposable blade scalpel on selected areas of the musical instruments. Following the sampling, the fragments were embedded into epoxy resin (Epofix Struers and Epofix Hardener, 15:2), and then cut into cross sections. The surface was then dry-polished using silicon-carbide fine sandpaper (500–8000 mesh) to obtain a flat surface. At least two layers of organic binders with a minimum thickness of 10 μm

Table 1. List of the violin makers, musical instruments and samples considered in this project.

	Period	Instrument Type	Instrument Name	Date	Instrument part	Sample Name
Francesco Ruggeri "il Per"	1630 – 1698	Cello	-	17th Century	Back plate	FR_c
Antonio Stradivari	1644 – 1737	Violin	Toscano	1690	Soundboard	AS_v
Lorenzo Storioni	1744 – 1816	Small Violin	-	1790	Rib	LS_v
Lorenzo Storioni	1744 – 1816	Small violin	Bracco	1793	Soundboard	LS_sv1
Lorenzo Storioni	1744 – 1816	Small violin	Bracco	1793	Soundboard	LS_sv2
Lorenzo Storioni	1744 – 1816	Small violin	Bracco	1793	Back plate	LS_sv3

were observed through an optical microscope in the coating systems of the five selected samples.

The micro-samples were analysed at the SISSI-Bio beamline (Chemical and Life Sciences branch) at Elettra Sincrotrone Trieste (Italy) [31]. Measurements were performed on the polished samples in terms of reflection geometry via infrared synchrotron radiation (IRSR) using a Bruker Vertex 70v interferometer coupled with a Hyperion 3000 microscope (Bruker Optik GmbH) and a single point mercury–cadmium–telluride (MCT) detector. A total of 512 scans were averaged in the acquisition spectral range of 4000–750 cm^{-1}, with a spectral resolution of 4 cm^{-1} and a scanner speed of 120 KHz. The size of the acquisition points was set at 10×30 μm by closing the knife-edge apertures of the vis-IR microscope according to the sample stratigraphy. The acquisition of 97 spectra was carried out in single-point mode and linear map mode with a vertical step size of 10 μm. For each sample, the background was acquired on a gold substrate using the same acquisition parameters. The reflection IR spectra were then transformed into absorbance spectra (as required for the interpretation of organic compounds) by applying Kramers–Kronig (KK) transformations using Opus 7.5 software.

The preliminary PCA data exploration was performed with a selection of 63 IR spectra (collected in linear map mode) from the IR dataset. Here, various spectral pre-treatments, namely, smoothing (Savitzky–Golay, 11 wavelengths gap size), first derivative (Savitzky–Golay, 11 wavelengths gap size and second-order polynomial), and mean centre, were applied. To develop the PLS–DA classification model, the entire IR dataset (97 spectra) was divided into a calibration set and a test set containing 71 (approx. 80 %) and 26 (20 %) spectra, respectively. The calibration set contained spectra referred to as samples AS_v, FR_c, LS_sv1, and LS_sv3, while the spectra collected on LS_sv2 and LS_v were used as the test set. Meanwhile, the models were cross-validated using the 'Venetian blinds' procedure with eight splits. The classification via PLS–DA involved the application of PLS regression to a *Y* dummy, completing a rotation of the projection to latent variables to obtain the maximum separation among the classes [32]. All the data analyses were performed in MATLAB (v. 2016a, MathWorks, Inc., Natick, MA, USA) using the PLS toolbox software package (ver. 8.5, Eigenvector Research, Inc., 130 USA).

3. RESULTS AND DISCUSSION

To obtain the maximum amount of information from the data and to reduce the impact of the non-diagnostic spectral features (e.g. signal noise and different baselines) the spectral range was initially reduced to a range of 3500–1000 cm^{-1} before being divided into six selected regions: 3500–3000 cm^{-1}, 3000–2700 cm^{-1}, 1800–1550 cm^{-1}, 1550–1450 cm^{-1}, 1460–1260 cm^{-1}, and 1250–1000 cm^{-1}. The reflection IR bands in the 3500–1000 cm^{-1} range of the most common organic materials documented in the finishing layers of historical violins are summarised in Table 2.

In the 3500–3000 cm^{-1} region, bands attributed to OH around 3500 cm^{-1} and to NH near 3300 cm^{-1} are generally present. However, the first overtone signal of the amide II is generally centred around 3080 cm^{-1} [35],[36]. Characteristic sharp, and often intense, signals produced by CH$_2$ and CH$_3$, can occur in the range of 3000–2700 cm^{-1}. These diagnostic bands are related to the tens of organic compounds variously used in painting and finishing wood surfaces, such as siccative oils,

Table 2. Wavenumber values between 3500 and 1000 cm^{-1} taken from the literature, together with their assignment, of the FTIR reflection bands produced by the materials identified in cross-sectioned samples. For the derivative bands, the value refers to the maximum of the band after the application of KK transformations. * Siccative oil and natural terpenic resins; ** non-treated wood.

Material	Wavenumber (cm^{-1})	Band shape	Assignment
Proteins [35],[36]	3330	Der	ν_{as}NH
	3080	Der	Overtone of amide II
	2960, 2875	Der	ν_{as}CH$_3$, ν_sCH$_3$
	2935, 2850	Der	ν_{as}CH$_2$, ν_sCH$_2$
	1650	Der	νC=O (amide I)
	1550	Der	δNH + νC-N (amide II)
	1450, 1400	Der	δCH
	1350–1200	Der	δNH + νC-N, δCH, δNH (amide III)
	1200–1000	Der	C-O
Oil-resin varnish * [33],[34]	2950, 2870	Der	ν_{as}CH$_3$, ν_sCH$_3$
	2930, 2850	Der	ν_{as}CH$_2$, ν_sCH$_2$
	1720–10	Der	νC=O
	1465–55, 1380	Der	δ_sCH$_2$, δ_{as}CH$_3$, δ_sCH$_3$
	1250, 1170, 1100	Der	νC-O
Wood ** [34],[37]	3450	Abs	νOH
	2940, 2900, 2840	Abs	ν_{as}CH$_2$, ν_{as}CH$_3$, ν_sCH$_2$,
	1735	Abs	νC=O
	1650	Abs	δOH
	1598, 1505	Abs	ν(aromatic ring)
	1465, 1430, 1380	Abs	δCH$_2$
	1330	Abs	δOH
	1280–1240	Abs	Guaiacyl ring vib., syringyl ring vib.
	1157	Der	ν_{as}C-O-C
	1115	Der	ν_{as} (glucose ring)
	1060, 1035	Der	ν_{as}C-O, ν_sC-O
Epoxy resin [38]-[40]	2960–2850	Der	νCH (arom. and aliph.)
	1610	Der	νC=C (aromatic ring)
	1510	Der	νC-C (aromatic ring)
	1250	Der	νC-O-C (oxirane group)
	1180	Der	Phenyl vib.
	1035	Der	νC-O-C (ether)

natural resins (vegetal and animal) [33],[34], and proteins, as well as the wood itself [34],[37]. At lower wavenumbers, the bands in the region from approximately 1730 to around 1690 cm^{-1} are attributed to the carbonyl stretching vibration of esters (e.g. from oils) and carboxylic acids (e.g. from resins) [33],[34], while those falling in the range of 1700–1600 cm^{-1}, mostly centred at around 1650 cm^{-1}, derive from the amide I of the proteinaceous materials (e.g. animal glue, casein) [35],[36]. Other marker bands related to these organic compounds can be identified in the fingerprint region, between 1450 and 1000 cm^{-1}, as shown in Table 2.

The presence of the epoxy resin used to embed the samples is clearly highlighted by the band at 1610 cm^{-1}, which is related to C=C (aromatic ring), the intense and sharp band at 1510 cm^{-1} C-C (aromatic ring), and by the bands between 1250 and 1000 cm^{-1} [38]-[40]. Signals from the epoxy resin can be expected in the spectra obtained from acquisition areas falling close to the upper or lower boundaries of the embedded sample.

In addition to the signals at high wavenumbers, the wooden substrate produces certain characteristic frequencies in the region between 1750 and 1550 cm⁻¹ and in the fingerprint region, as shown in Table 2.

3.1. PCA investigation

Figure 1 presents the results obtained via PCA in the six different selected spectral regions. Each object (i.e. each single spectrum) is classified and coloured in accordance with the position of the analytical spot in the coating system: epoxy resin (E), varnish (V), ground coat (G), and wood (W). Therefore, their assignment mainly reflects the distribution of the organic compounds in the samples. It is worth noting that the IR dataset was composed of spectra clearly related to a single organic material, indicating significant marker bands, together with spectra carrying signals produced by multiple layers (e.g. varnish + ground coat). These expected 'mixed' profiles originated from the acquisition areas at the interface between two adjacent layers with different compositions and were labelled as Mix 1 (varnish + epoxy resin), Mix 2 (varnish + ground coat), and Mix 3 (wood + ground coat).

The PC1 vs. PC2 scores plot, which related to the range at higher frequencies (Figure 1a), accounted for 86 % of the total variance. It is clear that the data exploration in this spectral region did not lead to a clear separation of the objects according to single organic materials. In the PC1 vs. PC2 scores plot (Figure 1b), which related to the range between 3000 and 2700 cm⁻¹ (85 % of total variance), the objects were scattered in the four quadrants. Nevertheless, it is possible to observe a cluster formed by objects related to the spectra labelled as wood (W), which were grouped in the fourth quadrant.
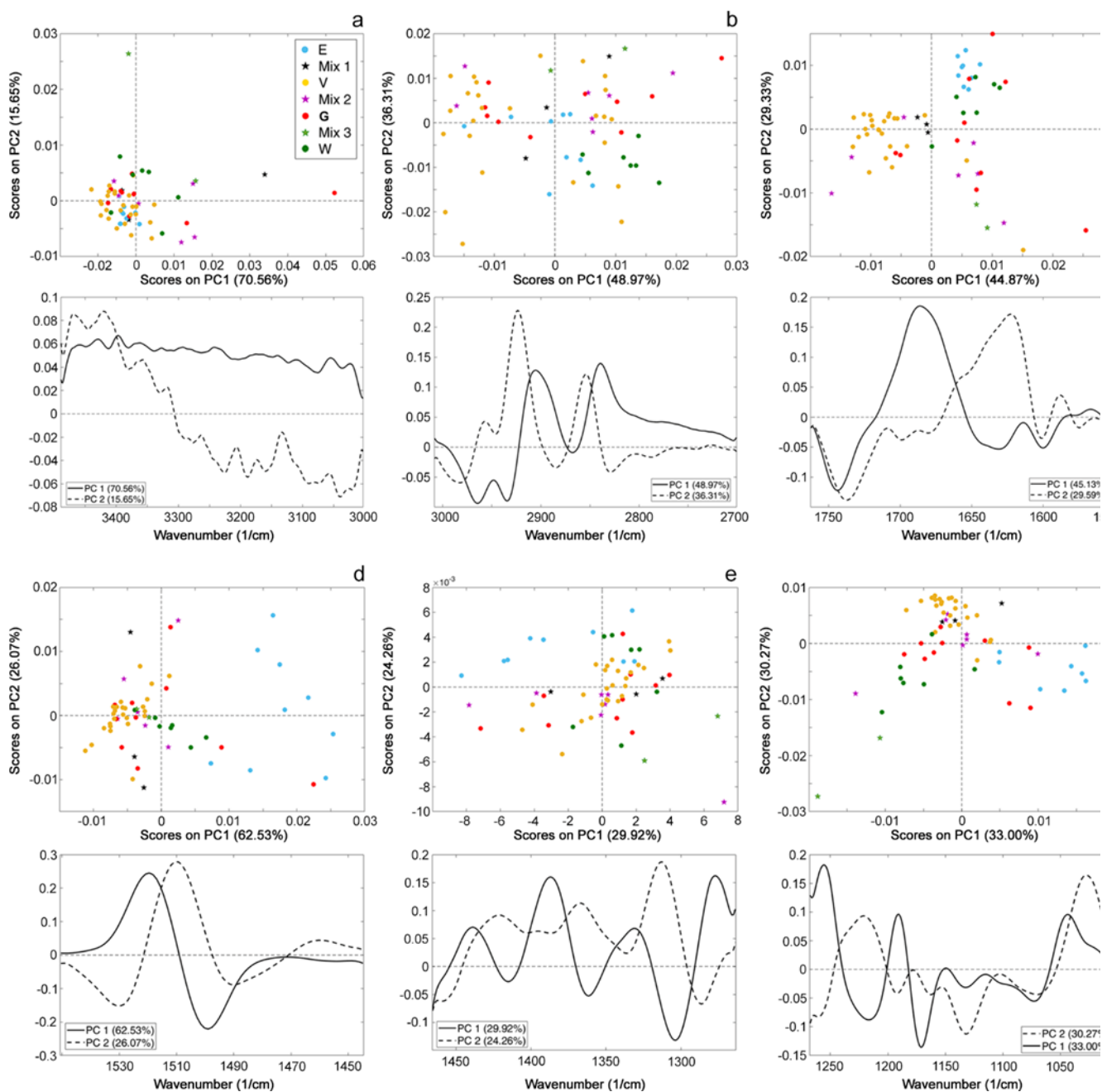

Figure 1. PCA results obtained in the six spectral regions selected in the range of 3500–1000 cm⁻¹. The scores and loadings plots are related to the following spectral regions: (a) 3500–3000 cm⁻¹, (b) 3000–2700 cm⁻¹, (c) 1800–1550 cm⁻¹, (d) 1550–1450 cm⁻¹, (e) 1460–1260 cm⁻¹, and (f) 1250–1000 cm⁻¹.
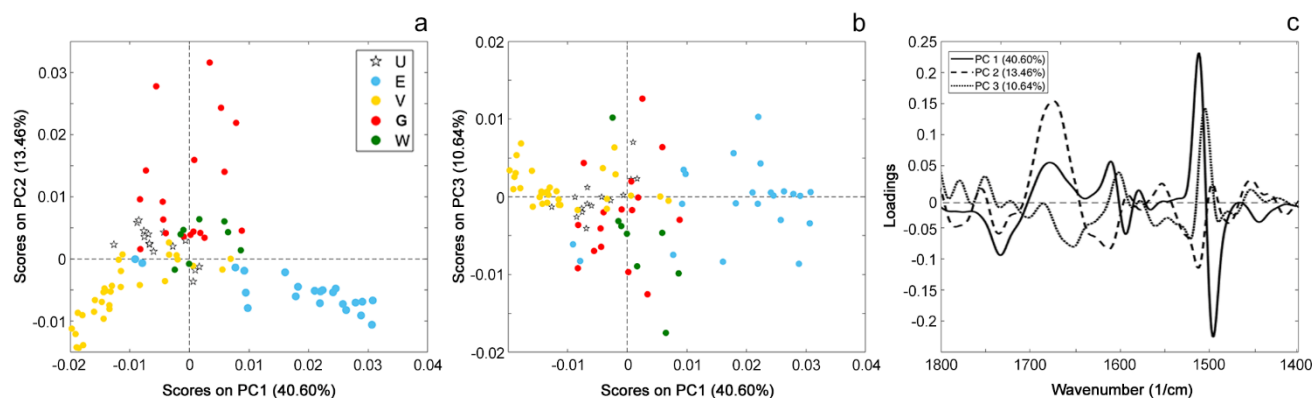
Figure 2. PCA results obtained in the region between 1800 and 1400 cm^{-1}: a) PC1 vs. PC2 scores plot; b) PC1 vs. PC3 scores plot; c) PC1, PC2, and PC3 loadings plot. E = epoxy resin, V = varnish, G = ground coat; W = wood; U = undefined.

The PC1 vs. PC2 scores plot related to the 1800–1550 cm^{-1} range (Figure 1c) accounted for 74 % of the total variance, and this appeared to be the most promising range for discriminating the objects. The spectra identified as V were mostly grouped in the PC1 negative area of the plot, with the spectra identified as E mainly in the first quadrant. Furthermore, the spectra collected at the interface between the V and E adjacent layers (i.e. Mix 1) assumed intermediate scores. The objects corresponding to the W layer were well grouped in the first quadrant and partly overlapped with the E objects. On the contrary, the G elements did not form a coherent cluster; rather they were heterogeneously scattered. Meanwhile, the objects identified as Mix 2 (i.e. the interface between V and G) were heterogeneously distributed in the negative PC2 portion, albeit that some were close to the V cluster, thus suggesting a higher influence of the varnish signature in the corresponding IR spectra. This object distribution was well explained by the corresponding loadings. The loadings plot highlighted the significant contribution of the negative signals between 1750 and 1700 cm^{-1}, which mainly characterised the PC1 and PC2 values of the V and Mix 1 groups. The positive signals between 1700 and 1600 cm^{-1}, respectively in the PC1 and PC2 loadings plot, characterised the objects labelled as E and W.

The scores plot of PC1 vs. PC2 related to the 1550–1450 cm^{-1} (Figure 1d) accounted for 89 % of the total variance. In this case, the objects that mostly differed along PC1 were V and E, albeit that the latter did not form a compact group but were distributed in the first and fourth quadrants. The spectra identified as W were close to each other and were distributed around the axes' origin. All the mixtures (i.e. the objects identified as spectra collected in the interface between two layers) did not exhibit a specific distribution. The PC1 values of the E objects were positive and higher than those related to other materials. This was due to the intense and sharp marker band of the epoxy resin centred at 1510 cm^{-1} (C-C, aromatic ring), which was confirmed by the strong signals observed in the region around 1500 cm^{-1} for both PC1 and PC2 loadings.

In the PC1 vs. PC2 scores plot in the range of 1460–1260 cm^{-1} (54 % of total variance), the picture was more chaotic (Figure 1e). Here, the objects did not form separate clusters, with the exception of E, which was mainly grouped in the second quadrant. The PC1 vs. PC2 scores plot related to the range of 1250–1000 cm^{-1} (Figure 1f) accounted for 63 % of the total variance. In this case, a partial separation of the objects according to the position of the analytical spot in the coating system was

identifiable, with most of the E, V, and W in the fourth, second and third quadrant, respectively.

On examining the different examined regions, the object distribution in the ranges of 1800–1550 cm^{-1} and 1550–1450 cm^{-1} appeared to be the most promising for discriminating the layers related to one single organic material and exhibiting significant marker bands. Meanwhile, the spectra acquired at the interface between two adjacent layers with different compositions did not always exhibit a clear trend.

Following this, further PCA was performed on the entire dataset (97 spectra) while considering the 1800–1400 cm^{-1} range and grouping all the 'mixed' profiles in a separate class, labelled as U (undefined). On examining the PC1 vs. PC2 scores plot (Figure 2a), it was clear that the objects associated with the varnish (V) spectral profiles were mostly grouped in the bottom left quarter of the plot, as these objects had both negative PC1 and negative PC2 scores. Meanwhile, most of the spectra identified as epoxy resin (E) corresponded to the objects grouped in the bottom right quarter, resulting from a positive PC1 combined with negative PC2 values. The objects corresponding to the spectra collected on the ground coat (G) did not form a sharp cluster in the PC1 vs. PC2 scores plot; however, all these objects were characterised by positive PC2 scores and most of them were well separated from the other layers. Wood (W) groups formed around the origin of the PC1 and PC2 axes close to the undefined layers (U).

In addition, the third PC (accounting for 11 % of the variance) was investigated. As Figure 2b shows, the previously identified groups were confirmed, even though some were more scattered or formed sub-groups.

From the loadings plot (Figure 2c), the signals corresponding to the bands used to detect epoxy resin, varnish, and ground coat (Table 2) – largely composed of proteins – appeared to be those that mostly influenced the spectra distribution in the groups according to the different materials constituting the layers. Here, it should be kept in mind that the spectra were transformed according to the first derivative, meaning the maximum of the diagnostic peaks was lost, while it did correspond to the inflection point of the loading profiles. As loadings can assume values from −1 to +1, the variables approaching extreme values in Figure 2c were those with a greater influence in constituting the PCs and, thus, were responsible for the spectra distribution in the score plots (Figure 2a,b).

Here, PC1 effectively discriminated the varnish (V) from the epoxy (E) spectra, mainly due to the signals around 1700 and 1510 cm^{-1}, while PC2 allowed for the discrimination of objects

Table 3. Figure of merit of the PLS–DA model related to the calibration (Cal), cross-validated (CV) and prediction (Pred) steps. Sens = sensitivity; Spec = specificity. E = epoxy resin, V = varnish, G = ground coat; W = wood; U = undefined.

	E	V	G	W	U
N (Cal)	17	20	12	4	18
N (Pred)	7	10	2	5	2
Sens (Cal)	1.00	0.90	0.83	1.00	0.94
Spec (Cal)	0.98	1.00	0.98	0.97	0.91
Sens (CV)	1.00	0.90	0.75	0.75	0.94
Spec (CV)	0.98	1.00	0.98	0.97	0.85
Sens (Pred)	**1.00**	**1.00**	0.50	0.60	**1.00**
Spec (Pred)	**0.78**	**0.91**	**1.00**	**1.00**	**1.00**

related to ground coat (G) due to the amide I signal (1665–1645 cm^{-1}).

3.2. PLS–DA classification model

The materials identified through the observation of each layer position in the stratigraphy and confirmed via PCA were used as classes (E, V, G, W and U), thus constituting the *a priori* information (Y) to build the PLS–DA classification model (Table 3) that has the capacity to predict the predominant materials in the layers based on the obtained spectral data (X).

The PLS–DA model was first calibrated, that is, a classification rule (equation) was established based on a representative set of samples. Following this, the model was internally validated via an iterative exclusion of part of the calibration set, that is, one out of the eight groups of samples (selected via the 'Venetian blinds' procedure) served as an internal test set, while the remaining data were used for the calibration. The results of the eight tests were then averaged and the constituent strategy that achieved the highest accuracy was selected. The prediction ability of the optimised model was then tested using an external test set.

The three steps of the model development (calibration, cross-validation, and prediction) were evaluated in terms of sensitivity and specificity. Here, sensitivity relates to the model's capacity to correctly recognise samples belonging to a specific class, while specificity relates to the model's capacity to correctly reject the samples belonging to all other classes. The internal validation (cross-validation) of the model performed well for most of the considered classes, achieving a sensitivity of over 0.90 and a specificity of over 0.85. However, with the G class, the sensitivity was 0.75, as four out of the 12 samples were misclassified as A (3) and W (1). This misclassification was expected since the *a priori* assigned classes related to the most present component in the layer; however, it is unrealistic to assume that each single layer is made up by one pure substance, which means each spectrum would potentially contain signals from different compounds. The model's prediction ability was optimal for the E and V classes, with a sensitivity of 1.00 and a specificity of over 0.78. However, while the specificity of the G and W classes reached the maximum level (1.00), the attendant sensitivity was poor. Here, one out of the two samples defined as ground coat was classified as undefined, while LS_v.25 and LS_v.26, which were defined as wood, were assigned to the epoxy class. The low performance of the prediction phase was largely related to the low number of spectra constituting some of the classes, mainly U and G. In fact, the misclassification of only one spectrum resulted in a specificity of 0.50 for the G class. However, the prediction phase presented the greatest strength of the developed model since this phase is missing in most heritage classification cases due to the difficulties in collecting data from different samples.

4. CONCLUSIONS

The investigation of precious and brittle micro-samples is a challenging task when thin layered systems such as those encountered in musical instruments are considered. In fact, to precisely characterise the attendant materials, an in-depth micro-invasive – if not micro-destructive – wide analytical campaign is generally needed. As such, how to employ SR–FTIR micro-spectroscopy to obtain hundreds of informative spectra on micro-samples without damaging the samples is a crucial aspect. Using SR at the SISSI-Bio beamline, it was possible to adopt reflection geometry with increased lateral resolution to take advantage of IRSR brightness to obtain better spectra (with higher signal-to-noise ratios) while avoiding contact with the cross sections and preserving the surfaces for further analyses.

A preliminary elaboration of the large SR–FTIR reflection dataset was performed using chemometric tools to obtain a rigorous picture of the IR results and to distinguish different material classes, previously selected in accordance with the position within the coating system of the analytical spot. Three additional mixed classes were identified at the interface between the layers. The PCA, which was performed on different spectral regions, confirmed the preliminary material assignment by highlighting clear sample groupings for varnish, ground coat, wood, and epoxy resin on the basis of their spectral features. Moreover, the explorative analysis confirmed that the spectra collected at the interfaces between different layers exhibited coherent signals produced by different materials. The PLS–DA classification model revealed the feasibility of the proposed methodological approach aimed at discriminating the constituent materials of bowed string instruments in a fast and rigorous way without the need to visually inspect a large number of spectra.

Further case studies are planned to expand the number of investigated historical instruments while considering other materials with characteristic spectral features. In addition, the method developed in this work will be tested on other datasets collected with different non-invasive analytical techniques (e.g. XRF, FTIR in reflection geometry) in relation to a large number of historical Cremonese musical instruments.

REFERENCES

[1] F. Caruso, D.F.C. Martino, S. Saverwyns, M.V. Bos, L. Burgio, C. Di Stefano, G. Peschke, E. Caponetti, Micro-analytical identification of the components of varnishes from South Italian historical musical instruments by PLM, ESEM–EDX, microFTIR, GC–MS, and Py–GC–MS, Microchem. J. 116 (2014), pp. 31-40. DOI: 10.1016/j.microc.2014.04.002

[2] S.L. Lämmlein, D. Mannes, B.V. Damme, F.W.M.R. Schwarze, I. Burgert, The influence of multi-layered varnishes on moisture protection and vibrational properties of violin wood, Sci. Rep. 9

(2019), 18611.
DOI: 10.1038/s41598-019-54991-5

[3] J.P. Echard, L. Bertrand, A. Von Bohlen, A.-S. Le Hô, C. Paris, L. Bellot-Gurlet, B. Soulier, A. Lattuati-Derieux, S. Thao, L. Robinet, B. Lavédrine, S. Vaiedelich, The nature of the extraordinary finish of Stradivari's instruments, Angew. Chem. Int. Ed. Engl. 49 (2009), pp. 197-201.
DOI: 10.1002/anie.200905131

[4] S. Tirat, I. Degano, J.P. Echard, A. Lattuati-Derieux, A. Lluveras-Tenorio, A. Marie, S. Serfaty, J.Y. Le Huérou, Historical linseed oil/colophony varnishes formulations: Study of their molecular composition with micro-chemical chromatographic techniques, Microchem. J. 126 (2016), pp. 200-213.
DOI: 10.1016/j.microc.2015.11.045

[5] A. Von Bohlen, S. Röhrs, J. Salomon, Spatially resolved element analysis of historical violin varnishes by use of µPIXE, Anal. Bioanal. Chem. 387 (2006), pp. 781-790.
DOI: 10.1007/s00216-006-0777-7

[6] F. Poggialini, G. Fiocco, B. Campanella, S. Legnaioli, V. Palleschi, M. Iwanicka, P. Targowski, M. Sylwestrzak, C. Invernizzi, T. Rovetta, M. Albano, M. Malagodi, Stratigraphic analysis of historical wooden samples from ancient bowed string instruments by laser induced breakdown spectroscopy, J. Cult. Herit. (2020), pp. 275-284.
DOI: 10.1016/j.culher.2020.01.011

[7] J. Nagyvary, R.N. Guillemette, C.H. Spiegelman, Mineral Preservatives in the Wood of Stradivari and Guarneri, PLoS ONE. 4 (2009), e4245.
DOI: 10.1371/journal.pone.0004245

[8] G. Fiocco, T. Rovetta, M. Malagodi, M. Licchelli, M. Gulmini, G. Lanzafame, F. Zanini, A. Lo Giudice, A. Re, Synchrotron radiation micro-computed tomography for the investigation of finishing treatments in historical bowed string instruments: Issues and perspectives, Eur. Phys. J. Plus. 133 (2018), p. 525.
DOI: 10.1140/epjp/i2018-12366-5

[9] G. Fiocco, T. Rovetta, M. Gulmini, A. Piccirillo, C. Canevari, M. Licchelli, M. Malagodi, Approaches for Detecting Madder Lake in Multi-Layered Coating Systems of Historical Bowed String Instruments, Coatings. 8 (2018), p. 171.
DOI: 10.3390/coatings8050171

[10] G. Fichera, T. Rovetta, G. Fiocco, G. Alberti, C. Invernizzi, M. Licchelli, M. Malagodi, Elemental analysis as statistical preliminary study of historical musical instruments, Microchem. J. 137 (2018), pp. 309-317.
DOI: 10.1016/j.microc.2017.11.004

[11] J.P. Echard, B. Lavédrine, Review on the characterisation of ancient stringed musical instruments varnishes and implementation of an analytical strategy, J. Cult. Herit. 9 (2008), pp. 420-429.
DOI: 10.1016/j.culher.2008.03.005

[12] B.H. Tai, Stradivari's varnish: A review of scientific findings - Part II, Journal of the Violin Society of America 22 (2009), pp. 1-31.

[13] B.H. Tai, Stradivari's varnish: A review of scientific findings - Part I., Journal of the Violin Society of America 21 (2007), pp. 119-144.

[14] T. Rovetta, C. Invernizzi, G. Fiocco, M. Albano, M. Licchelli, M. Gulmini, G. Alf, D. Fabbri, A.G. Rombolà, M. Malagodi, The case of Antonio Stradivari 1718 ex-San Lorenzo violin: History, restorations and conservation perspectives, J. Archaeol. Sci. Rep. 23 (2019), pp. 443-450.
DOI: 10.1016/j.jasrep.2018.11.010

[15] J.V.D. Weerd, R.M.A. Heeren, J.J. Boon, Preparation methods and accessories for the infrared spectroscopic analysis of multi-layer paint films, Stud. Conserv. 49 (2004), p. 193.
DOI: 10.1179/sic.2004.49.3.193

[16] C. Invernizzi, G. Fiocco, M. Iwanicka, M. Kowalska, P. Targowski, B. Blümich, C. Rehorn, V. Gabrielli, D. Bersani, M. Licchelli, M. Malagodi, Non-invasive mobile technology to study the stratigraphy of ancient Cremonese violins: OCT, NMR-MOUSE, XRF and reflection FT-IR spectroscopy, Microchem. J.

155 (2020), 104754.
DOI: 10.1016/j.microc.2020.104754

[17] L. Bertrand, L. Robinet, S.X. Cohen, C. Sandt, A.-S.L. Hô, B. Soulier, A. Lattuati-Derieux, J.P. Echard, Identification of the finishing technique of an early eighteenth century musical instrument using FTIR spectromicroscopy, Anal. Bioanal. Chem. 399 (2010) pp. 3025-3032.
DOI: 10.1007/s00216-010-4288-1

[18] G. Sciutto, P. Oliveri, S. Prati, E. Catelli, I. Bonacini, R. Mazzeo, A multivariate methodological workflow for the analysis of FTIR chemical mapping applied on historic paint stratigraphies, Int. J. Anal. Chem. 2017 (2017) pp. 1-12.
DOI: 10.1155/2017/4938145

[19] G. Fiocco, T. Rovetta, C. Invernizzi, M. Albano, M. Malagodi, M. Licchelli, A. Re, A. Lo Giudice, G.N. Lanzafame, F. Zanini, M. Iwanicka, P. Targowski, M. Gulmini, A micro-tomographic insight into the coating systems of historical bowed string instruments, Coatings. 9 (2019) p. 81.
DOI: 10.3390/coatings9020081

[20] F. Caruso, S. Orecchio, M.G. Cicero, C.D. Stefano, Gas chromatography–mass spectrometry characterization of the varnish and glue of an ancient 18th century double bass, J. Chromatogr. A. 1147 (2007) pp. 206-212.
DOI: 10.1016/j.chroma.2007.02.048

[21] J.P. Echard, C. Benoit, J. Peris-Vicente, V. Malecki, J. Gimeno-Adelantado, S. Vaiedelich, Gas chromatography/mass spectrometry characterization of historical varnishes of ancient Italian lutes and violin, Anal. Chim. Acta. 584 (2007) pp. 172-180.
DOI: 10.1016/j.aca.2006.10.048

[22] S. Grassi, G. Fiocco, C. Invernizzi, T. Rovetta, M. Albano, P. Davit, M. Gulmini, C. Stani, L. Vaccari, M. Licchelli, M. Malagodi, Managing complex synchrotron radiation FTIR micro-spectra from historic bowed musical instruments by chemometrics, Proc. of 2019 IMEKO TC4 International Conference on Metrology for Archaeology and Cultural Heritage, Florence, Italy, Dec. 04-06, 2019, pp. 114-119.
DOI:

[23] G. Fiocco, C. Invernizzi, S. Grassi, P. Davit, M. Albano, T. Rovetta, C. Stani, L. Vaccari, M. Malagodi, M. Licchelli, M. Gulmini, Reflection FTIR spectroscopy for the study of historical bowed string instruments: Invasive and non-invasive approaches, Spectrochim. Acta A 245 (2021) p. 118926.
DOI: 10.1016/j.saa.2020.118926

[24] K. Sano, S. Arrighi, C. Stani, D. Aureli, F. Boschin, I. Fiore, V. Spagnolo, S. Ricci, J. Crezzini, P. Boscato, M. Gala, A. Tagliacozzo, G. Birarda, L. Vaccari, A. Ronchitelli, A. Moroni, S. Benazzi, The earliest evidence for mechanically delivered projectile weapons in Europe, Nat. Ecol. Evol. 3 (2019) pp. 1409-1414.
DOI: 10.1038/s41559-019-0990-3

[25] K. Jalovec, Italian Violin Makers, Crown Publishers, New York, 1957.

[26] G. Sciutto, P. Oliveri, S. Prati, M. Quaranta, S. Lanteri, R. Mazzeo, Analysis of paint cross-sections: A combined multivariate approach for the interpretation of µATR-FTIR hyperspectral data arrays, Anal. Bioanal. Chem. 405 (2012) pp. 625-633.
DOI: 10.1007/s00216-011-5680-1

[27] S. Prati, G. Sciutto, I. Bonacini, R. Mazzeo, New frontiers in application of FTIR microscopy for characterization of cultural heritage materials, Top. Curr. Chem. 374 (2016) p. 26.
DOI: 10.1007/s41061-016-0025-3

[28] N. Salvadó, S. Butí, M.J. Tobin, E. Pantos, A.J. Prag, T. Pradell, Advantages of the use of SR-FT-IR microspectroscopy: Applications to cultural heritage, Anal. Chem. 77 (2005) pp. 3444-3451.
DOI: 10.1021/ac050126k

[29] S. Wold, K. Esbensen, P. Geladi, Principal component analysis, Chemometr. Intell. Lab. 2 (1987) pp. 37-52.
DOI: 10.1016/0169-7439(87)80084-9

[30] R. Bro, A.K. Smilde, Principal component analysis, Anal. Methods. 6 (2014) pp. 2812-2831.
DOI: 10.1039/c3ay41907j

[31] S. Lupi, A. Nucara, A. Perucchi, P. Calvani, M. Ortolani, L. Quaroni, M. Kiskinova, Performance of SISSI, the infrared beamline of the ELETTRA storage ring, J. Opt. Soc. Am. 24 (2007) p. 959.
DOI: https://doi.org/10.1364/josab.24.000959

[32] P. Oliveri, M. Forina, Data analysis and chemometrics, in: Chemical Analysis of Food: Techniques and Applications. Yolanda Pico (editor). Academic Press, Cambridge, 2012, ISBN 9780123848635, pp. 25-48.

[33] C. Invernizzi, A. Daveri, T. Rovetta, M. Vagnini, M. Licchelli, F. Cacciatori, M. Malagodi, A multi-analytical non-invasive approach to violin materials: The case of Antonio Stradivari 'Hellier' (1679), Microchem. J. 124 (2016) pp. 743-750.
DOI: 10.1016/j.microc.2015.10.016

[34] C. Invernizzi, A. Daveri, M. Vagnini, M. Malagodi, Non-invasive identification of organic materials in historical stringed musical instruments by reflection infrared spectroscopy: A methodological approach, Anal. Bioanal. Chem. 409 (2017) pp. 3281-3288.
DOI: 10.1007/s00216-017-0296-8

[35] C. Invernizzi, T. Rovetta, M. Licchelli, M. Malagodi, Mid and near-infrared reflection spectral database of natural organic materials in the cultural heritage field, Int. J. Anal. Chem. 2018 (2018) pp. 1-16.
DOI: 10.1155/2018/7823248

[36] F.N. Fu, D.B. Deoliveira, W.R. Trumble, H.K. Sarkar, B.R. Singh, Secondary structure estimation of proteins using the amide III region of Fourier transform infrared spectroscopy: Application to analyze calcium-binding-induced structural changes in calsequestrin. Appl. Spectrosc. 48 (1994) pp. 1432-1441.
DOI: 10.1366/0003702944028065

[37] T. Poli, O. Chiantore, M. Nervo, A. Piccirillo, Mid-IR fiber-optic reflectance spectroscopy for identifying the finish on wooden furniture, Anal. Bioanal. Chem. 400 (2011) pp. 1161-1171.
DOI: 10.1007/s00216-011-4834-5

[38] M.G. González, J.C. Cabanelas, J. Baselga, Applications of FTIR on epoxy resins - identification, monitoring the curing process, phase separation and water uptake, in: Infrared Spectroscopy - Materials Science, Engineering and Technology. T. Theophile (editor). IntechOpen, London, 2012, ISBN 978-953-51-0537-4, pp. 261-284.

[39] R.E. Smith, F.N. Larsen, C.L. Long, Epoxy resin cure. II. FTIR analysis, J. Appl. Polym. 29 (1984) pp. 3713-3726.
DOI: 10.1002/app.1984.070291207

[40] H. Panda, Epoxy Resins Technology Handbook (Manufacturing Process, Synthesis, Epoxy Resin Adhesives and Epoxy Coatings), Asia Pacific Business Press, New Delhi, 2019, ISBN 978-8178331829.